processes

MDPI

Article

Nonlinear Adaptive Generalized Predictive Control for PH Model of Nutrient Solution in Plant Factory Based on ANFIS

Yonggang Wang [1], Ning Zhang [1,*], Chunling Chen [1], Yingchun Jiang [2] and Tan Liu [1]

[1] College of Information and Electronic Engineering, Shenyang Agricultural University, Shenyang 110866, China; wygvern@syau.edu.cn (Y.W.); chenchunling@syau.edu.cn (C.C.); liutan0822@syau.edu.cn (T.L.)
[2] College of Engineering, Shenyang Agricultural University, Shenyang 110866, China; jyclg@syau.edu.cn
* Correspondence: zn2021@stu.syau.edu.cn; Tel.: +86-155-2440-8900

Abstract: A plant factory is typically considered to be an exceedingly advanced product management system characterized by higher crop yields and better quality control. The pH value of the nutrient solution is crucial for determining the health and productivity of crops. However, the nutrient solution process exhibits inherent complexity, such as parameters uncertainty, multi-disturbances, and strong nonlinearity. Therefore, the traditional control method cannot meet the necessary requirements. The main objective of this paper is to address the issues of parameter uncertainty, strong nonlinearity, and multiple disturbances in the regulation process of the nutrient solution while achieving accurate control of the nutrient solution pH in a plant factory. This is performed so that a dynamic model of a nutrient solution for pH is developed and a nonlinear adaptive controller is presented, which comprises a linear adaptive generalized predictive controller, a nonlinear adaptive generalized predictive controller, and a switching mechanism. The parameters of the controller are adjusted by generalized predictive control (GPC) laws. In this approach, an adaptive neuro-fuzzy inference system (ANFIS) is used to estimate the unmodeled dynamics to depress the influence of nonlinearity on the system. The experiments show that the mean errors and standard errors for gain-scheduling the proportional-integral-derivative (PID) control strategy are 0.1388 and 0.4784, respectively. The mean errors and standard errors for the nonlinear adaptive controller are 0.1046 and 0.3009, respectively. Simulation results indicate that the presented method can acquire a better control effect in the case of various complex situations. Therefore, by achieving precise control of the pH value, it is possible to provide a suitable growth environment for crops, promoting healthy crop growth and increasing crop yield.

Keywords: plant factory; nutrient solution; pH control; nonlinear adaptive control; generalized predictive control (GPC); adaptive neuro-fuzzy inference system (ANFIS)

Citation: Wang, Y.; Zhang, N.; Chen, C.; Jiang, Y.; Liu, T. Nonlinear Adaptive Generalized Predictive Control for PH Model of Nutrient Solution in Plant Factory Based on ANFIS. *Processes* **2023**, *11*, 2317. https://doi.org/10.3390/pr11082317

Academic Editors: Valentina E. Balas and Rajeeb Dey

Received: 8 June 2023
Revised: 17 July 2023
Accepted: 28 July 2023
Published: 2 August 2023

1. Introduction

A plant factory is one of the most advanced development technologies of modern agriculture; it is characterized by higher unit output, a higher degree of production automation, a higher resource utilization rate, and green health [1–3]. A nutrient solution is an indispensable source of nutrients for crop growth in plant factories that is designed to provide suitable ionic elements for crop growth. Hydroponics is a system in which the nutrient solution supplies water, nutrients, and oxygen to crops instead of natural soil so that crops can grow healthily during the life cycle [4,5]. The advantage of hydroponic systems is that they can avoid continuous cropping obstacles and diseases that often occur in soil cultivation [6,7]. The four essential indicators of nutrient solutions for plant factories are pH, EC, temperature, and oxygen. Significantly, the pH value of the nutrient solution is crucial for determining the health and productivity of crops. The pH value is a measure of the acidity or alkalinity of a solution, representing the concentration of hydrogen ions (H^+)

in the solution. Different crops in plant factories have specific pH requirements for optimal nutrient absorption. Moreover, maintaining the appropriate pH level in nutrient solutions ensures that crops can readily absorb essential nutrients [8,9]. However, it is a challenging task for the pH control problem due to the strong nonlinearity, parameters uncertainty, and multi-disturbances for the nutrient solution process.

Many forms of pH modeling for nutrient solutions have been proposed, which can be represented by the continuous stirred tank reactor (CSTR) model [10]. The typical pH general model has been developed from the perspective of these mechanisms [11]. The abovementioned mathematical model can be described by the dynamic model and static nonlinear model. The dynamic model describes the dynamic change of the concentration of each chemical component in CSTR. The nonlinear model reflects the balance of chemical components in a system at equilibrium. A bilinear model of a pH model was approached [12]. A pH model was presented by solving a non-linear algebraic equations system based on chemical equilibrium equations, mass balances, and the electroneutrality principle [13]. To accurately predict the behavior of pH processes in tubular mixers and in-line systems, a distributed parameter model has been proposed in [14]. It should be noted that an accurate mathematical model was difficult to obtain owing to a mismatch in model parameters. In addition, there are also limitations when applying pH modeling in plant factories. These include the significant upfront investment required for system installation and the continuous requirement for monitoring system operations, particularly in terms of electricity supply.

Over the past few years, many academics have put forward control strategies, such as robust control [15,16], feedforward control [17], adaptive control [18–20], fuzzy control [21–23], optimal control [24,25], and so on. However, the control strategy proposed in aforementioned papers can only deal with systems whose dynamics are linearly characteristic. Therefore, the classical linear control strategy can only achieve a good control effect within a small range of working points for weak nonlinear systems. The controller design for the pH value of nutrient solutions encounters a significant challenge due to its inherent complexity. There are three main reasons, as follows:

(1) The nutrient solution process can be described as a dynamic system with strong nonlinearity characterized by significant gain fluctuation at different working points. In particular, the sensitivity of pH changes is very large when the pH reaches the neutral point. A small input change may cause a great output change [26].

(2) Furthermore, the pH of nutrient solutions is severely influenced by multi-disturbances and parameters uncertainty, such as fluctuations of fertilizer flow and irrigation water flow, instable factors including acid concentration, and the alkali concentration of the feed solution [27].

(3) The pH value of a nutrient solution is highly dynamic and primarily influenced by the absorption of ions by crops roots, the hydrolysis of carbon dioxide (CO_2), and the loss of H^+ ions, resulting in elevated cation levels. As a result, the pH variation in the nutrient solution becomes intricate and challenging to control.

Artificial intelligence theories, such as neural networks, are utilized as a promising approach for control problems. Because neural networks can approximate any continuous functions between finite-dimensional spaces and arbitrary accuracy, many scholars have tried to apply neural networks to nonlinear control. To stabilize certain types of nonlinear strict-feedback systems with uncertain dynamics while considering full-state constraints, an adaptive neural network control method was investigated [28]. A nonlinear multi-agent adaptive neural network controller with constraints was presented [29]. Aiming at a specific class of nonlinear systems that feature multiple-input and multiple-output (MIMO) variables, an adaptive output feedback fault-tolerant controller based on a neural network was proposed [30]. A control strategy based on neural networks was proposed for adaptive decoupling of nonlinear systems to enhance evaporation efficiency [31]. A feedback-based adaptive controller based on a neural network was presented for improved control performance [32].

By building upon the control strategy presented in references [33–36], a nonlinear adaptive control scheme utilizing ANFIS is proposed to address the control problem related to regulating the pH value of nutrient solutions. This article makes several contributions to the field, including:

(1) To achieve precise control of pH value and ensure that the pH value of the nutrient solution is suitable for crop growth, a dynamic model for nutrient solution pH is established based on the actual conditions of the factory.

(2) To the best of our knowledge, there is a significant lack of research exploring the potential application of the nonlinear generalized prediction adaptive control method on the basis of ANFIS in pH control of nutrient solutions. The control method comprises a linear adaptive generalized predictive controller, a nonlinear adaptive generalized predictive controller, and a switching mechanism. The parameters of the controller are adjusted by GPC laws. In this approach, ANFIS is used to estimate the unmodeled dynamics to depress the influence of nonlinearity on the system.

2. Process Description of the Nutrient Solution

The model and control of the research are experimented on in the plant factory (Figure 1a) located at Haicheng Sanxing Ecological Agriculture Co., Ltd. in Liaoning Province. The size of the plant factory is 16 m in length, 6 m in width, and 3 m in height. The interior of the plant factory (Figure 1b) has three cultivation racks, which are 14 m long, 0.3 m wide, and 0.5 m high. The nutrient solution process system in the plant factory is shown in Figure 1c. From left to right, the four tanks contain fertilizer, acid, alkali, and a mixed nutrient solution, and the volumes of the four tanks are 300 L, 300 L, 300 L, and 500 L, respectively. The initially composition of the fertilizer includes $Ca(NO_3)_2$ $4H_2O$—315 mg/L; KNO_3—712 mg/L; $MgSO_4$ $7H_2O$—542 mg/L; and $(NH_4)_2HPO_4$—301 mg/L. For pH control, the acid solution uses HCL—0.36 mol/L, while the alkaline solution uses NaOH—0.1 mol/L. The transmission pipe (Figure 1d) of the nutrient solution system is made of polyvinyl chloride (PVC), with a diameter of 8 cm.

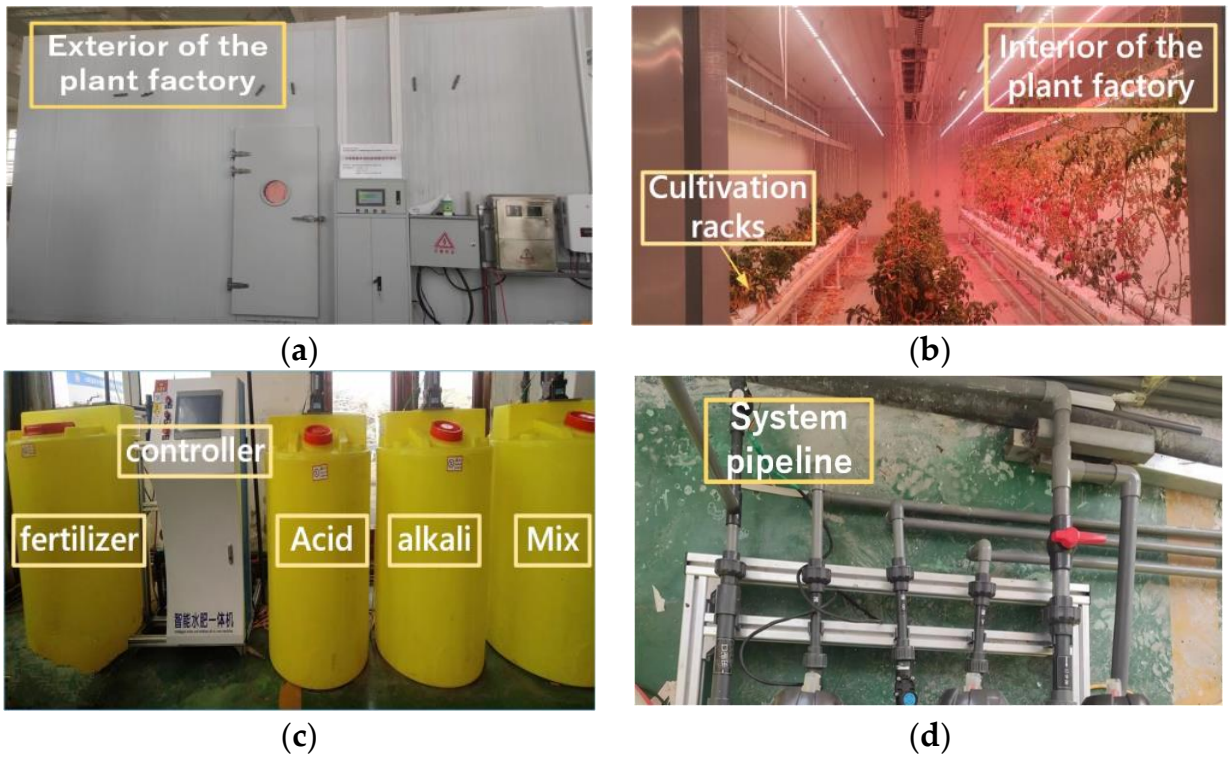

Figure 1. Architecture diagram of the interior (**a**) and exterior (**b**) of the plant factory. Architecture diagram of the nutrient solution system (**c**). Pipeline architecture diagram of the nutrient solution system (**d**).

A construction diagram of the nutrient solution system is displayed, as shown in Figure 2. The system takes place at the reaction center and has four inputs and one output. The inputs are acid solution, alkali solution, fertilizer solution, and irrigation water. The output is mixed nutrient solution, which is sent to the cultivation rack under pressure by the fertilization pump. The symbols in Figure 2 are explained as follows: GL—filter; JL—metering pump; PH—sensor; d_1, d_2, d_3, d_4—electromagnetism valve.

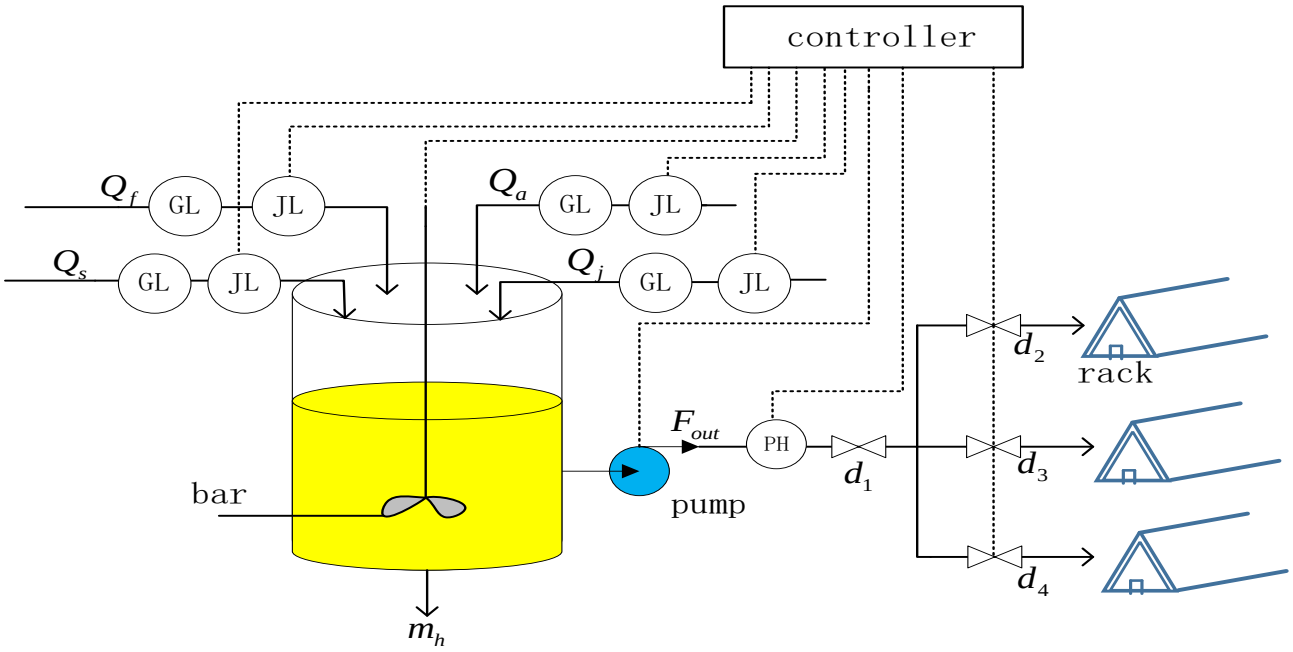

Figure 2. Construction diagram of the nutrient solution system.

In the actual configuration process of the nutrient solution, the controller regulates the input flow rate of acid liquid (Q_a), alkali liquid (Q_j), fertilizer liquid (Q_f), and irrigation water (Q_s) by the metering pumps (JL). In order to be well mixed for the nutrient solution, the stirring device is activated when the liquid flows into the mixing tank (m_h). The pH value is detected by the sensor. After comparing the measurement value of pH with the setpoint value, the controller adjusts each input flow and configures the qualified nutrient solution. Finally, the qualified nutrient solution is extracted through the fertilization pump supplied to the crops of the plant factory through the electromagnetism valve.

3. pH Model of the Nutrient Solution

Figure 3 displays the diagrammatic sketch of the pH of nutrient solution systems. The dynamic model of the pH of nutrient solutions and the continuous stirred tank reactor (CSTR) model are similar. The feed liquids include acid liquid, lye liquid, fertilizer liquid, and irrigation water. The pH model of the nutrient solution is established according to the ionization balance. It is assumed that complete ionization of acid and alkali is accomplished in the mixed tank, which is represented by Equations (1) and (2).

$$V\frac{dC_1}{dt} = Q_a X_a - \left[Q_a + Q_j + Q_f + Q_S\right]C_1 \quad (1)$$

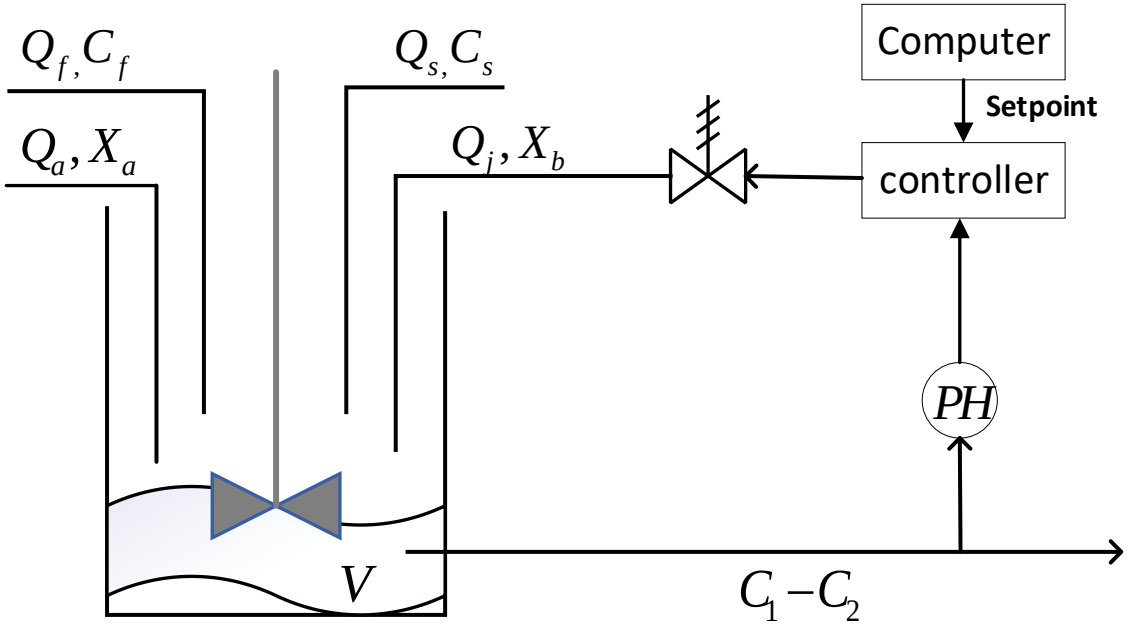

Figure 3. Diagrammatic sketch of the pH of the nutrient solution system.

In Equation (1), C_1 is the hydrogen ion concentration (i.e., $C_1 = H^+$), V is the reactor volume, Q_a is the inflow acid flow, X_a is the inflow acid concentration, Q_j is the inflow alkali flow, Q_f is the inflow of fertilizer, and Q_S is the inflow water flow.

$$V\frac{dC_2}{dt} = Q_j X_b + Q_f C_f + Q_S C_S - \left[Q_a + Q_j + Q_f + Q_S\right]C_2 \tag{2}$$

In Equation (2), C_2 is the concentration of hydroxide ions (i.e., $C_2 = OH^-$), C_f is the inflow fertilizer concentration, and C_S is the inflow water concentration.

Make $C_1 = x_1$, $C_2 = x_2$, $Q_a = F(t)$, $Q_j = u(t)$ and define $\Delta x(t) = x_1(t) - x_2(t)$.

$$\Delta\dot{x} = \frac{(X_a - y)F(t) - (X_b + y)U(t) - \left(Q_f + Q_s\right)y - Q_f C_f - Q_s C_s}{V} \tag{3}$$

In Equation (3):

$$\Delta x(t) = H^+ - OH^- = 10^{-pH} - 10^{-pH-14} = 10^{-pH} - 10^{-pH}.K_w \tag{4}$$

where $K_w = 10^{-14}$ is the hydroelectric balance constant.

Defining pH = y from Formula (4), it can be solved that:

$$y(t) = log_{10}\frac{-\Delta x(t) + (\Delta x(t)^2 + 4K_w)^{\frac{1}{2}}}{2K_w} \tag{5}$$

4. Dynamic Characteristics

The dynamic model of the pH of the nutrient solution is denoted in Equations (3)–(5). Table 1 contains the parameters utilized in the simulations of the model. To design a control strategy of the system, the dynamic characteristics, parameters uncertainty, and nonlinearity are discussed in this section.

Table 1. Simulation parameter table.

Parameter	Meaning	Value Range	Unit
V	reactor volume	500	L
Kw (25 °C)	water ionization constant	10^{-14}	
Q_a	inflow acid flow	1.0	L/min
X_a	inflow acid concentration	0.36	mol/L
X_b	inflow alkali concentration	0.1	mol/L
Q_f	inflow of fertilizer	0.5	L/min
C_f	inflow fertilizer concentration	0.1	mol/L
Q_s	inflow water flow	1.5	L/min
C_s	inflow water concentration	0.1	mol/L

4.1. Parameters Uncertainty

It is significant to notice that the model parameters are constant for many ideal assumptions in establishing the pH model of the nutrient solution. Although it is possible to avoid significant fluctuations by controlling the quantity of nutritional elements through the monitoring system, there are many uncertainties for some parameters in the actual system of the nutrient solution as time goes on. For example, X_a, X_b, and Q_a vary with time in Equation (3). Subsequently, parameters uncertainty experiments are discussed below.

The initial value of the system is u = 3.6 L/min; y = 7 and the input and output of the system are not changed in the experimental process. The parameter X_a is adjusted from the initial value of 0.36 mol/L to 0.32 mol/L, 0.34 mol/L, 0.38 mol/L, and 0.40 mol/L for investigating the output response of the system. The results of the experiment are depicted in Figure 4.

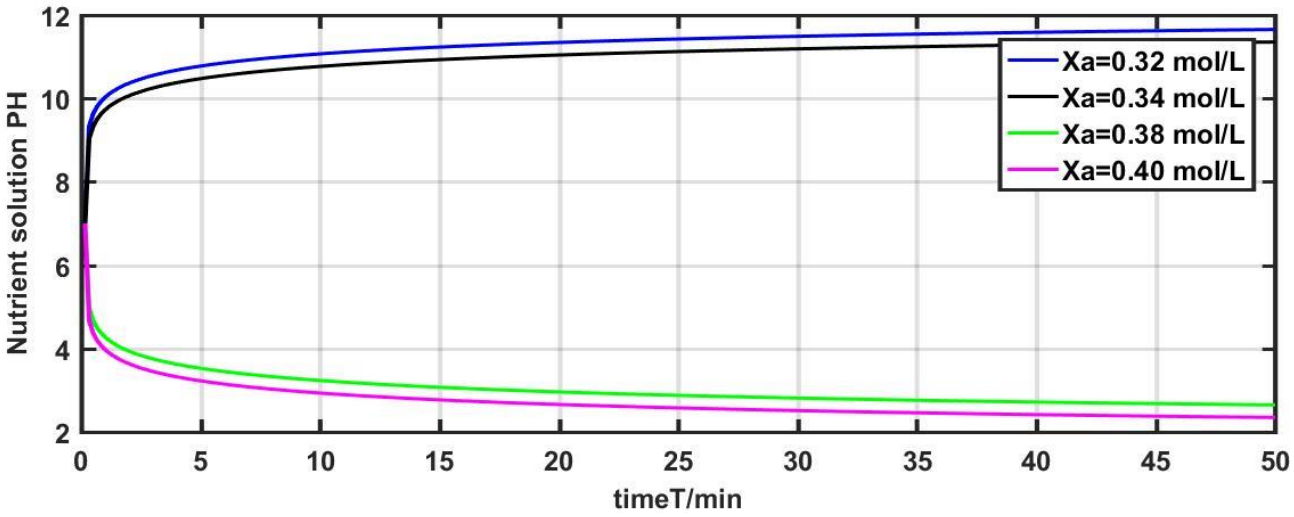

Figure 4. Uncertainty of inflow acid concentration X_a.

The results show that the pH value has fluctuated dramatically with the change of the model parameter X_a. As shown in Figure 4, the pH value changed from 7 to 11.5 at X_a = 0.32 mol/L and varied from 7 to 11 at X_a = 0.34 mol/L. The pH value of the nutrient solution changed from 7 to 3 at X_a = 0.38 mol/L and varied from 7 to 2.3 at X_a = 0.4 mol/L.

The model parameter X_b is adjusted from the initial value of 0.1 mol/L to 0.08 mol/L, 0.09 mol/L, 0.11 mol/L, and 0.12 mol/L for investigating the output response of the system. The results of the experiment are depicted in Figure 5.

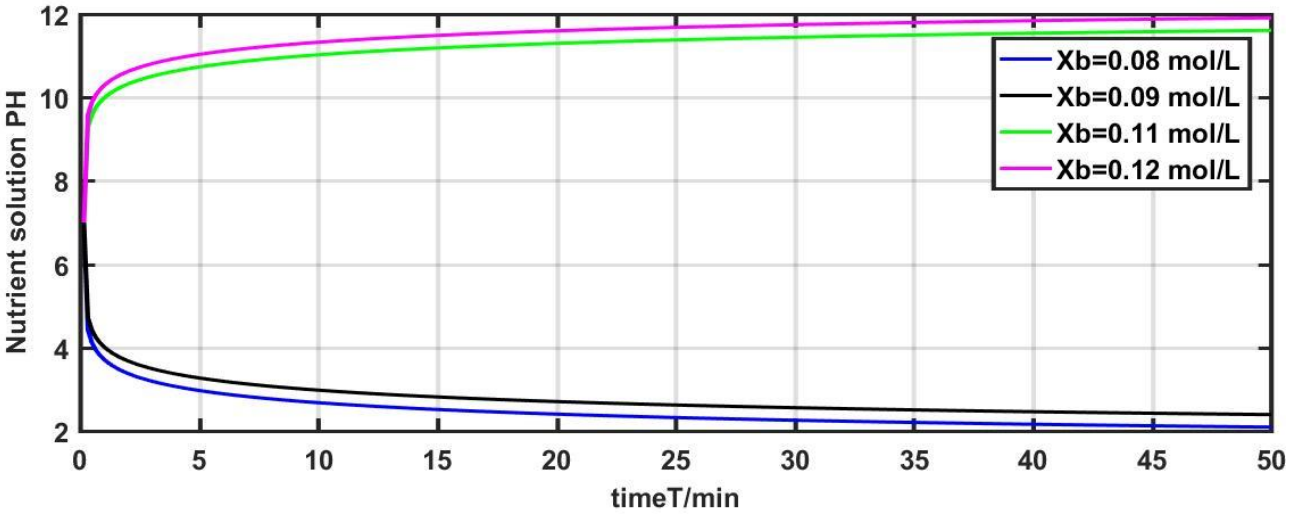

Figure 5. Uncertainty of inflow alkali concentration X_b.

The results show that the pH value has changed significantly with the modification of the model parameter X_b simultaneously. As shown in Figure 5, the pH value changed from 7 to 2 at X_b = 0.08 mol/L and varied from 7 to 2.5 at X_b = 0.09 mol/L. The pH value of the nutrient solution changed from 7 to 11.5 at X_b = 0.11 mol/L and varied from 7 to 12 at X_b 0.12 mol/L.

The model parameter Q_a is adjusted from the initial value of 1 L/min to 0.8 L/min, 0.9 L/min, 1.1 L/min, and 0.13 L/min for investigating the output response of the system. The results of the experiment are depicted in Figure 6.

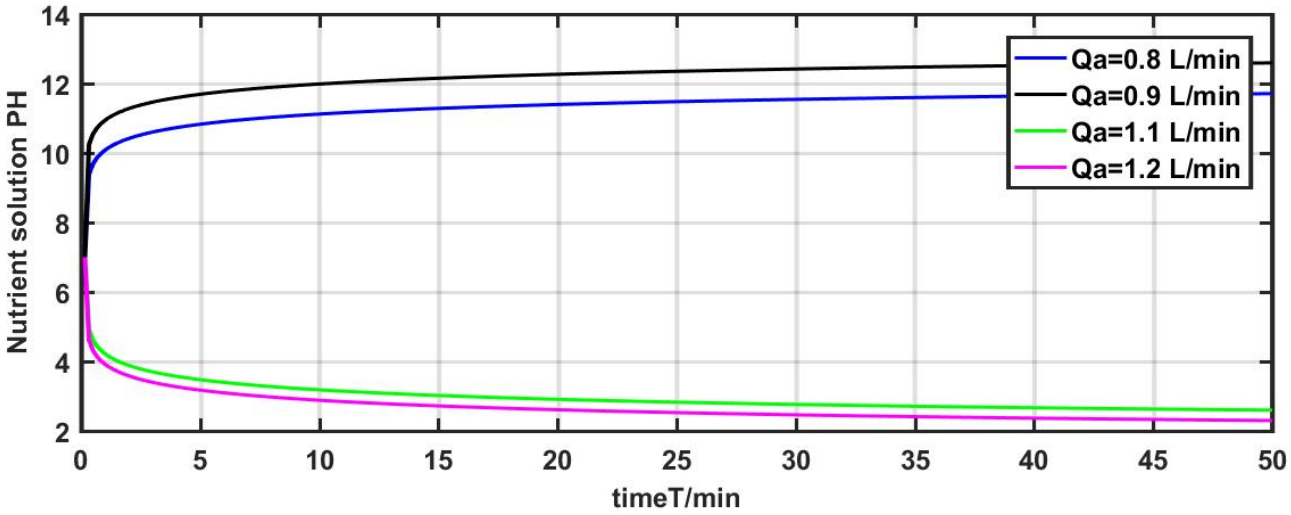

Figure 6. Uncertainty of inflow acid flow uncertainty Q_a.

The results show that the pH value has a similar response with the change of the model parameter Q_a. As shown in Figure 6, the pH value of the nutrient solution changed from 7 to 12 at Q_a = 0.8 L/min and varied from 7 to 11 at Q_a = 0.9 L/min. The pH value of the nutrient solution changed from 7 to 3 at Q_a = 1.1 L/min and varied from 7 to 2.3 at Q_a = 1.2 L/min.

It is evident from the aforementioned three experiments that the pH value of the system has changed remarkably with the slight modification of the model parameters X_a, X_b, and Q_a. Furthermore, fluctuations of fertilizer flow and irrigation water flow also affect the dynamic characteristics of the pH of the nutrient solution. Therefore, it is necessary to depress the influence of multi-disturbances and parameters uncertainty on the system.

4.2. Nonlinearity of the System

Figure 7 shows the titration curve for the pH value, which describes the static input–output relationship of the system [37]. It is seen clearly that the pH of the solution has a small change where the reaction process is far away from the neutral point (pH = 7), even if a large amount of alkali liquid is added. However, the sensitivity of the pH becomes very large when the reaction process is around the neutral point. Adding a small amount of alkali liquid can cause a large change in the pH value. As shown in Figure 7, the pH of the solution system exhibits strong output multiplicity. The static curve increases from nearly 0 degrees to nearly 90 degrees and then reduces from almost 90 degrees to almost 0 degrees. Based on the concept in [38], the pH of the nutrient solution system has strong static nonlinearity.

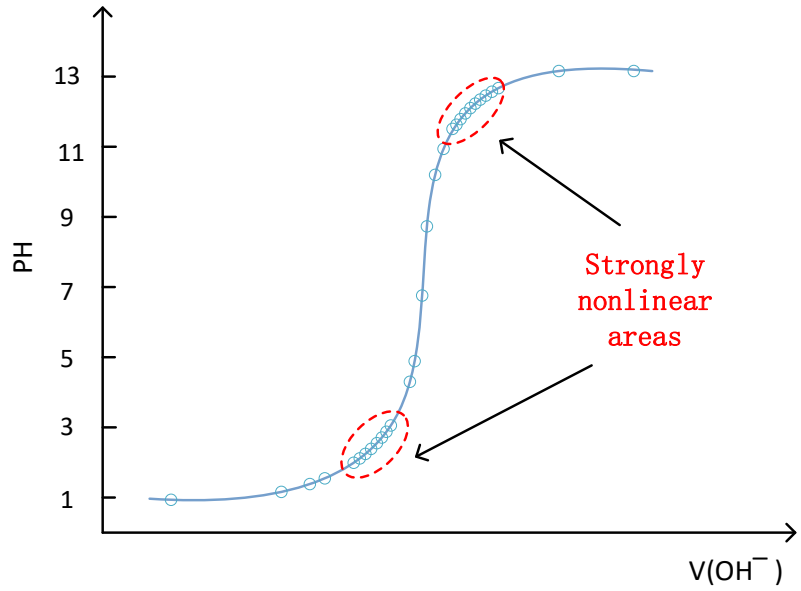

Figure 7. pH titration curve of the nutrient solution.

In order to further illustrate the nonlinear characteristic of the nutrient solution system, this paper uses the gap metric method to measure the nonlinear strength of the pH of the nutrient solution [39]. The working space of the nutrient solution system M can be meshed with N_g working points in the working space. The linearization model at the i point and the j point of the system is L_iM, L_jM in the working area. Select the largest gap m as the nonlinearity measure of the system in its working area. The degree of nonlinearity can be expressed using the following formula:

$$m = \max_{i,j=1,,, N_g} \{\delta(L_iM, L_jM)\} \tag{6}$$

By following the steps for calculating the gap metric, one can obtain a measure of nonlinearity:

(1) By leveraging existing knowledge about the system, distribute N_g working points in the whole working space.

(2) Linearize the nonlinear systems and obtain linearized models corresponding to all working points.

(3) Calculate the gap metric values between the N_g linearized models, and the $N_g \times N_g$ gap-matrix is computed.

(4) Compare the matrix components one by one and use the largest element to represent the nonlinearity measure of the system in the working space.

The pH of the nutrient solution system is divided within the range of pH $\in$ [2–12]. The number of working points is N_g = 1100, where 1100 linear models can be obtained by linearizing the dynamics of the nonlinear system near these points. Gap metric values are

calculated for 1100 different linear systems, and the maximum gap among the $N_g \times N_g$ gaps is selected as the nonlinearity degree. The gaps are displayed in Figure 8.

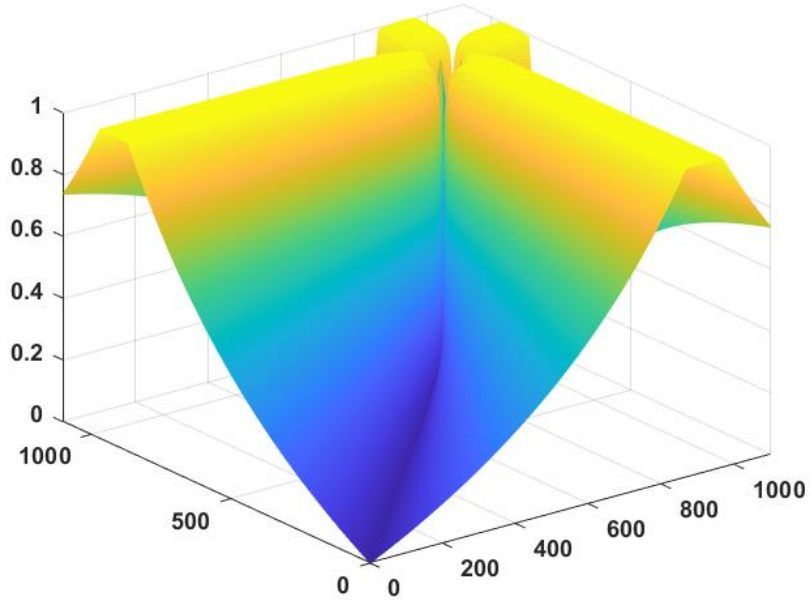

Figure 8. Nonlinear measurement curve of the nutrient solution system.

The results show that the nonlinearity measure $m = 1$. Furthermore, there are great differences in characteristics of the nutrient solution system at different working points in the given working space. Thus, as the system exhibits significant nonlinearity in its working range, a nonlinear control approach is required.

5. Nonlinear Adaptive Control Based on ANFIS

5.1. Nonlinear Generalized Predictive Controller

In the actual nutrient solution control system, there are different dynamic characteristics for the different working points. Therefore, this paper adopts a multi-model method that used different nonlinear models to describe the nutrient solution system at different working points.

Near the i working point, the system can be described as follows [40]:

$$A_i\left(z^{-1}\right)y(k) = B_i\left(z^{-1}\right)u(k-1) + v_i(k-1) \qquad i = 1, 2, \cdots, m \tag{7}$$

where m is the number of known working points. $A_i\left(z^{-1}\right)$ and $B_i\left(z^{-1}\right)$ are polynomials about z^{-1}, for which the formulas are as follows:

$$A_i\left(z^{-1}\right) = 1 + a_{i1}z^{-1} + \ldots + a_{in_a}z^{-n_a}$$

$$B_i\left(z^{-1}\right) = b_{i0} + b_{i1}z^{-1} + \cdots + b_{in_b}z^{-n_b}$$

$v_i(k-1) = f[y(k-1), \cdots y(k-n_a), u(k-1), \cdots u(k-n_b-1)]$ represents the high-order nonlinear term.

The generalized predictive performance index is introduced in the following function:

$$J = \sum_{j=1}^{N}\left[y(k+j) - r_{ij}w(k+j) + S_{ij}\left(z^{-1}\right)v_i(k+j-1)\right]^2 + \sum_{j=1}^{N_u}\lambda_{ij}u(k+j-1)^2 \tag{8}$$

where $w(k) \in R$ is the known reference input, N, N_u denote the length of the prediction and control horizon, respectively, λ_{ij} is the weighted coefficient of the control quantity, $S_{ij}(z^{-1})$ is the weighted polynomial about z^{-1}, and r_{ij} is the weighted constant.

To predict j steps ahead, consider the following two Diophantine equations:

$$1 = E_{ij}\left(z^{-1}\right)A_i\left(z^{-1}\right) + z^{-j}F_{ij}\left(z^{-1}\right) \tag{9}$$

$$E_{ij}\left(z^{-1}\right)B_i\left(z^{-1}\right) = G_{ij}\left(z^{-1}\right) + z^{-j}H_{ij}\left(z^{-1}\right) \tag{10}$$

where $E_{ij}(z^{-1}) = e_{i0} + e_{i1}z^{-1} + \cdots + e_{i(j-1)}z^{-j+1}$, $F_{ij}(z^{-1}) = f_0^{ij} + f_1^{ij}z^{-1} + \cdots + f_{n_a-1}^{ij}z^{-n_a+1}$, $G_{ij}(z^{-1}) = g_{i0} + g_{i1}z^{-1} + \cdots + g_{i(j-1)}z^{-j+1}$, $H_{ij}(z^{-1}) = h_0^{ij} + h_1^{ij}z^{-1} + \cdots + h_{n_b-1}^{ij}z^{-n_b+1}$.

The j step output prediction can be obtained from Equations (7), (9) and (10), which is given by:

$$y(k+j) = G_{ij}\left(z^{-1}\right)u(k+j-1) + F_{ij}\left(z^{-1}\right)y(k) + H_{ij}\left(z^{-1}\right)u(k-1) + E_{ij}\left(z^{-1}\right)v_i(k+j-1) \tag{11}$$

Substituting Equation (11) into (8) and selecting a weighted polynomial $S_{ij}(z^{-1})$ to make:

$$\left[E_{ij}\left(z^{-1}\right) + S_{ij}\left(z^{-1}\right)\right]v_i(k+j-1) = M_{ij}\left(z^{-1}\right)v_i(k-1),\ j = 1, \cdots, N \tag{12}$$

where $M_{ij}(z^{-1}) = m_{i0} + m_{i1}z^{-1} + \cdots + m_{in_m}z^{-n_m}$, and then yields:

$$J = \sum_{j=1}^{N}\left[G_{ij}\left(z^{-1}\right)u(k+j-1) + F_{ij}\left(z^{-1}\right)y(k) + H_{ij}\left(z^{-1}\right)u(k-1) + M_{ij}\left(z^{-1}\right)v_i(k-1) - r_{ij}w(k+j)\right]^2 + \sum_{j=1}^{N_u}\lambda_{ij}u(k+j-1)^2 \tag{13}$$

Expressing the performance index in Equation (13) in the form of a vector as follows:

$$J = [G_iU + H_iu(k-1) + F_iy(k) + M_iv_i(k-1) - R_iW]^T[G_iU + H_iu(k-1) + F_iy(k) + M_iv_i(k-1) - R_iW] + U^T\lambda_iU$$

where,

$$U = \begin{bmatrix} u(k) \\ \vdots \\ u(k+N_u-1) \end{bmatrix},\ W = \begin{bmatrix} w(k+1) \\ \vdots \\ w(k+N) \end{bmatrix},\ H = \begin{bmatrix} H_{i1}(z^{-1}) \\ \vdots \\ H_{iN}(z^{-1}) \end{bmatrix},\ F = \begin{bmatrix} F_{i1}(z^{-1}) \\ \vdots \\ F_{iN}(z^{-1}) \end{bmatrix}$$

$$G_i = \begin{bmatrix} g_{i0} & & & \\ g_{i1} & g_{i0} & & \\ \vdots & \vdots & & \\ g_{i(N_u-1)} & g_{i(N_u-2)} & \cdots & g_{i0} \\ \vdots & \vdots & & \vdots \\ g_{i(N-1)} & g_{i(N-2)} & \cdots & g_{i(N-N_u)} \end{bmatrix},\ M_i = \begin{bmatrix} M_{i1}(z^{-1}) \\ \vdots \\ M_{iN}(z^{-1}) \end{bmatrix},\ R_i = diag\left[r_{ij}\right]$$

$\lambda_i = diag[\lambda_{i1}, \cdots, \lambda_{iN_u}],\ j = 1, \cdots, N.$

Minimizing the performance index in Equation (13) yields the nonlinear generalized predictive control law as follows:

$$U = \left(G_i{}^TG_i + \lambda_i\right)^{-1}G_i{}^T[R_iW - F_iy(k) - H_iu(k-1) - M_iv_i(k-1)] \tag{14}$$

The defined $(G_i{}^T G_i + \lambda_i)^{-1} G_i{}^T$ first row is $p_i{}^T = [p_i \cdots p_{iN}]$; the nonlinear generalized predictive control law is obtained as follows, and the nonlinear controller structure is shown in Figure 9:

$$H_{ic}\left(z^{-1}\right)u(k) = P_i\left(z^{-1}\right)w(k+N) - F_i\left(z^{-1}\right)y(k) - M_{ic}\left(z^{-1}\right)v_i(k-1) \tag{15}$$

where, $P_i(z^{-1}) = p_{iN}r_{iN} + p_{i(N-1)}r_{i(N-1)}z^{-1} + \cdots + p_{i1}r_{i1}z^{-N+1}$, $F_{ic}(z^{-1}) = \sum_{k=1}^{N} p_{ik}F_{ik}(z^{-1})$, $H_{ic}(z^{-1}) = 1 + z^{-1}\sum_{k=1}^{N} p_{ik}H_{ik}(z^{-1})$, $M_{ic}(z^{-1}) = \sum_{k=1}^{N} p_{ik}M_{ik}(z^{-1})$ and $\deg[F_{ic}(z^{-1})] = n_a - 1$. $\deg\left[H_{ic}(z^{-1})\right] = n_b$.

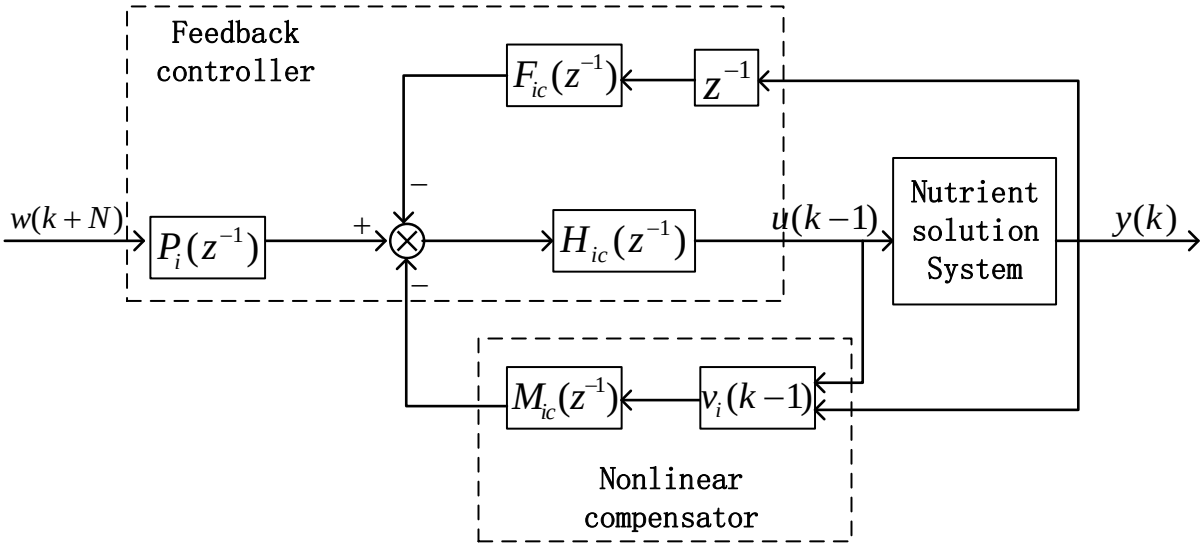

Figure 9. Nonlinear controller structure.

Substituting Equation (15) into the system Equation (7), the equation for the closed-loop system can be derived as follows:

$$\begin{aligned}&[A_i(z^{-1})H_{ic}(z^{-1}) + z^{-1}B_i(z^{-1})F_{ic}(z^{-1})]y(k)\\ &= z^{-1}B_i(z^{-1})P_i(z^{-1})w(k+N) + [H_{ic}(z^{-1}) - z^{-1}B_i(z^{-1})M_{ic}(z^{-1})]v_i(k-1)\end{aligned} \tag{16}$$

To guarantee the stability of the closed-loop system, appropriate selection of weighting constants λ_{ij} needs to be preset (note that $H_{ic}(z^{-1})$ and $F_{ic}(z^{-1})$ are related to λ_{ij}):

$$T_i\left(z^{-1}\right) = A_i\left(z^{-1}\right)H_{ic}\left(z^{-1}\right) + z^{-1}B_i\left(z^{-1}\right)F_{ic}\left(z^{-1}\right) \neq 0, |z| \geq 1 \tag{17}$$

To remove the steady-state error and unmodeled dynamic on the system, appropriately selecting weighting polynomials r_{ij}, $S_{ij}(z^{-1})$ satisfies the following equation (note that $P_i(z^{-1})$ is related to r_{ij} and $M_{ic}(z^{-1})$ are related to $S_{ij}(z^{-1})$):

$$A_i(1)H_{ic}(1) + B_i(1)F_{ic}(1) = B_i(1)P_i(1) \tag{18}$$

$$H_{ic}(1) = B_i(1)M_{ic}(1) \tag{19}$$

If the nonlinear term is not considered, the linear control strategy can be seen in Figure 10, and the linear generalized predictive controller law is obtained by Equation (20):

$$H_{ic}\left(z^{-1}\right)u(k) = P_i\left(z^{-1}\right)w(k+N) - F_{ic}\left(z^{-1}\right)y(k) \tag{20}$$

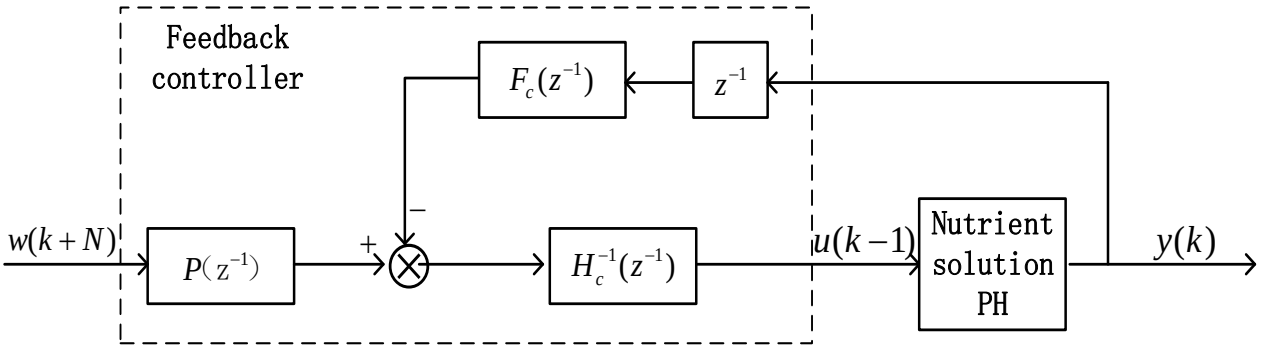

Figure 10. Linear controller structure.

5.2. Estimation Model and Corresponding Adaptive Controller

In practical nutrient solution systems, the parameters of the model always change with various factors, such as influent acid and alkali concentration. Therefore, it is necessary to update the coefficient in Equation (7) at different working conditions.

From Equation (7), the parameters of the nonlinear system can be identified as follows:

$$y(k) = X_i{}^T(k-1)\theta_i + v_i(k-1) \tag{21}$$

where, $\theta_i = [a_{i1}, \cdots, a_{in_a}, b_{i0}, \cdots, b_{in_b}]^T$, $X_i(k-1) = [-y(k-1), \cdots, -y(k-in_a), u(k-1), \cdots, u(k-in_b-1)]^T$.

The definition of the linear estimation model M_{i1} is as follows:

$$\hat{y}_1(k) = X_i{}^T(k-1)\hat{\theta}_{i1}(k-1) \tag{22}$$

where $\hat{\theta}_{i1}(k)$ represents the estimated value of the parameter at time k based on the linear model (22) and $\hat{\theta}_{i1}(k)$ can be determined by the following algorithm:

$$\hat{\theta}_{i1}(k) = \hat{\theta}_{i1}(k-1) + \frac{\mu_{i1}(k)X_i(k-1)e_{i1}(k)}{1 + X_i{}^T(k-1)X_i(k-1)} \tag{23}$$

$$\mu_{i1}(k) = \begin{cases} 1, & if\ |e_{i1}(k)| > 4\Delta \\ 0, & else \end{cases} \tag{24}$$

$$e_{i1}(k) = y(k) - \hat{y}_1(k) = y(k) - X_i{}^T(k-1)\hat{\theta}_{i1}(k-1) \tag{25}$$

From Equation (20), the linear generalized predictive adaptive controller C_{11} can be obtained as follows:

$$\hat{H}_{ic1}\left(z^{-1}\right)u(k) = \hat{P}_{i1}\left(z^{-1}\right)w(k+N) - \hat{F}_{ic1}\left(z^{-1}\right)y(k) \tag{26}$$

Because the neural networks can more accurately approximate the original nonlinear system (7), ANFIS is used to estimate the nonlinear terms to enhance the control effectiveness of the system. The model M_{i2} based on the nonlinear estimation term is defined as:

$$\hat{y}_2(k) = X_i{}^T(k-1)\hat{\theta}_{i2}(k-1) + \hat{v}_i(k-1) \tag{27}$$

where $\hat{\theta}_{i2}(k)$ is the estimate based on the nonlinear estimation model for parameter θ_i at k time. The parameter identification algorithm of $\hat{\theta}_{i2}(k)$ is as follows:

$$\hat{\theta}_{i2}(k) = \hat{\theta}_{i2}(k-1) + \frac{\mu_{i2}(k)X_i(k-1)e_{i2}(k)}{1 + X_i{}^T(k-1)X_i(k-1)} \tag{28}$$

$$\mu_{i2}(k) = \begin{cases} 1, & if\ |e_{i2}(k)| > 4\Delta \\ 0, & else \end{cases} \tag{29}$$

$$e_{i2}(k) = y(k) - \hat{y}_2(k) = y(k) - X_i{}^T(k-1)\hat{\theta}_{i2}(k-1) - \hat{v}_i(k-1) \tag{30}$$

The nonlinear adaptive control law is presented as follows, corresponding to the ANFIS nonlinear estimation model C_{12}. The structure of this nonlinear adaptive controller is shown in Figure 11.

$$\hat{H}_{ic2}\left(z^{-1}\right)u(k) = \hat{P}_{i2}\left(z^{-1}\right)w(k+N) - \hat{F}_{ic2}\left(z^{-1}\right)y(k) - \hat{M}_{ic2}\left(z^{-1}\right)\hat{v}_i(k-1) \tag{31}$$

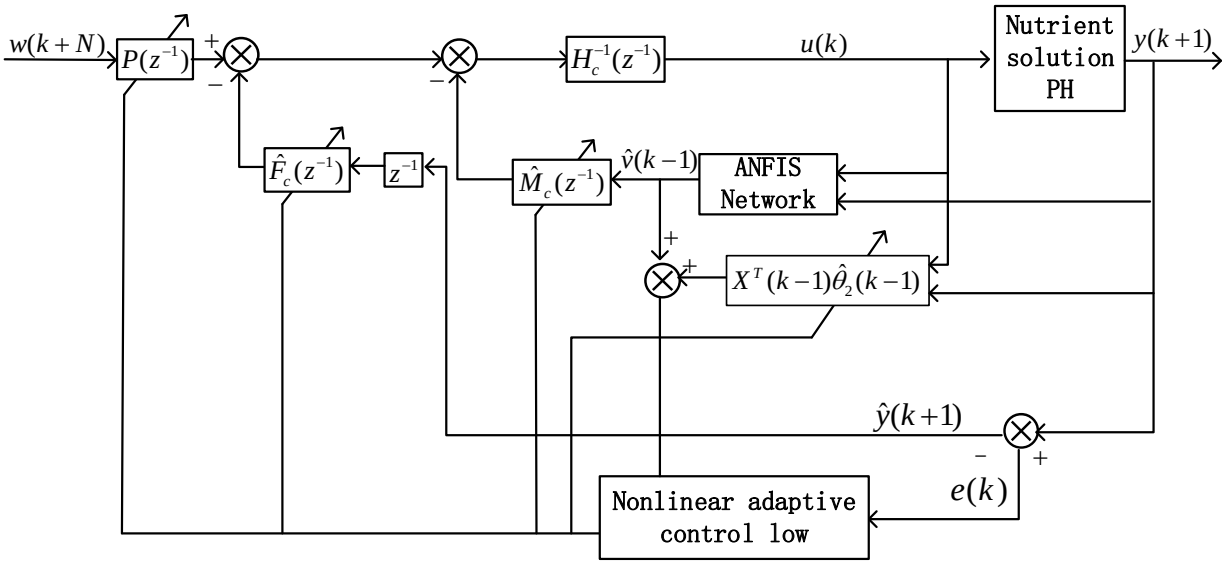

Figure 11. Nonlinear adaptive controller structure.

5.3. Switching System Design

In the nutrient solution system, if the nonlinear term $\hat{v}_i(k-1)$ is small, a linear adaptive controller can be employed for guaranteeing the stability of the closed-loop system. However, if the estimated value of the nonlinear term $\hat{v}_i(k-1)$ is large, the control performance is greatly depressed using the linear adaptive controller alone. Therefore, a nonlinear adaptive controller is needed to minimize the effect of the nonlinear term on the system. However, the nonlinear adaptive controller cannot guarantee the stability of the closed-loop system. Therefore, a switching mechanism is proposed to enhance the characteristics of the control system and to ensure the stability of the closed-loop system, simultaneously. The switching mechanism utilizing multiple models is depicted in Figure 12. The switching criterion is defined by Equations (32) and (33):

$$J_{ij}(k) = \sum_{l=1}^{k} \frac{\mu_{ij}(l)e_{ij}^2(l)}{2(1+X^T(l-1)X(l-1))} + c\sum_{l=k-T+1}^{k}\left(1-\mu_{ij}(l)\right)e_{ij}^2(l)\ (i=1,\ldots m; j=1,2) \tag{32}$$

where T is a positive int and $c \geq 0$ is a constant. $j=1$ denotes linear and $j=2$ denotes nonlinear. At any time k, $J_{\xi\rho}(k)$, $(1 \leq \xi \leq m, 1 \leq \rho \leq 2)$ is the minimum switching function, which is defined as follows:

$$J_{\xi\rho}(k) = \min_{1\leq i\leq m, j=1,2}\left\{J_{ij}(k)\right\} \tag{33}$$

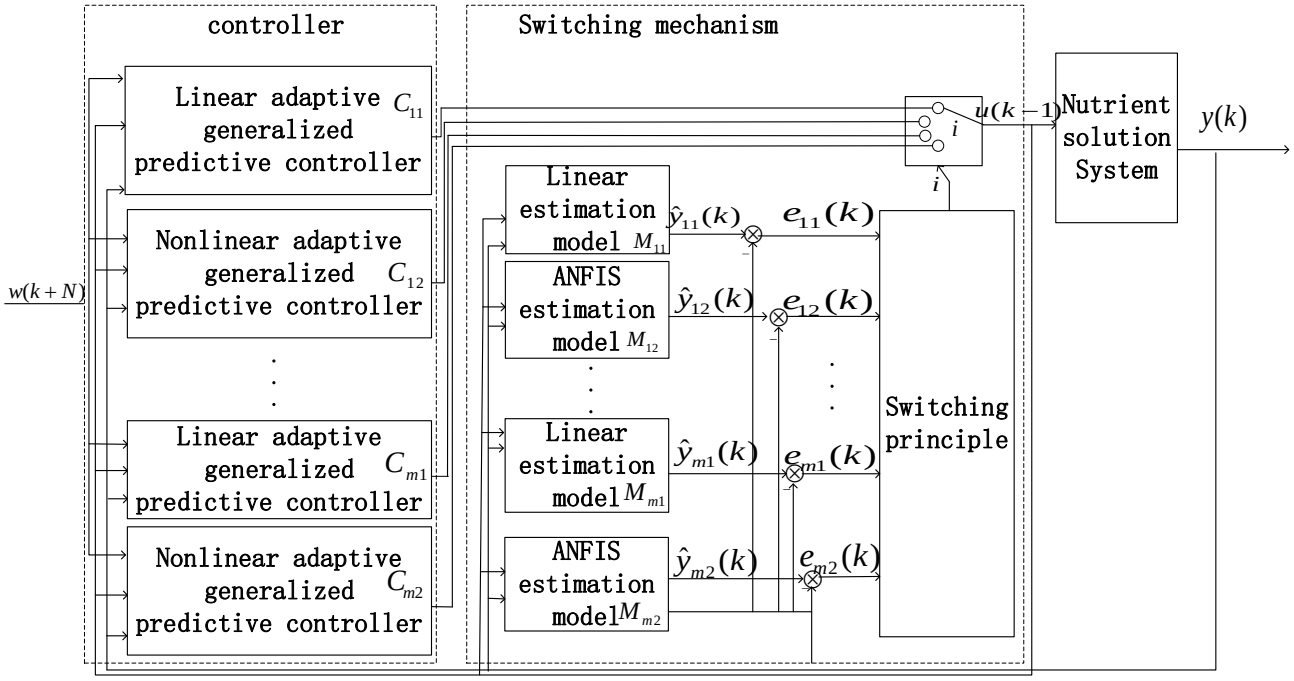

Figure 12. Switching mechanism based on multiple models.

Then, the system will select the corresponding model $M_{\xi\rho}$. The controller $C_{\xi\rho}$ will output counterpart values to the model $M_{\xi\rho}$. These output values will be used as the control input $u(k)$ for the k time system. At each time, the system's output is predicted by both the linear model (22) and the nonlinear model (27), and the parameters of both models are simultaneously renewed using the input–output data of the system.

5.4. ANFIS for Unmodeled Dynamics

It is a commonly accepted fact that neural networks can approximate nonlinear terms with arbitrary precision. Therefore, the unmodeled dynamics of the nutrient solution process are estimated using ANFIS. The ANFIS network structure diagram is shown in Figure 13.

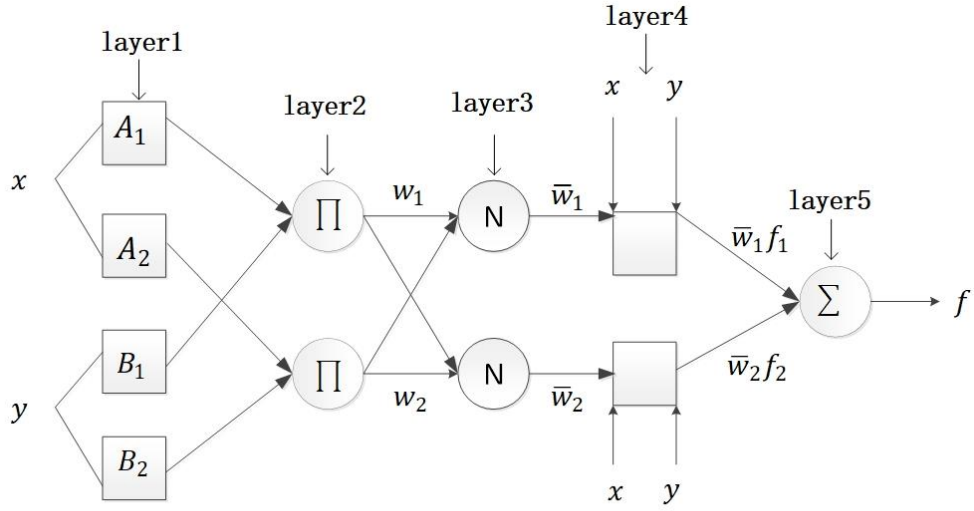

Figure 13. ANFIS network structure diagram.

The ANFIS has five layers, and the output of each layer can be obtained by the following relations.

Layer[1]: Each square node q indicated by A_q or B_q in layer[1] has a node function as follows:

$$O_{1,q} = \mu A_q(x),\ q = 1,2 \tag{34}$$

$$O_{1,q} = \mu B_q(y),\ q = 1,2 \tag{35}$$

$O_{1,q}$ is the membership function of the fuzzy set A_q or B_q, which can be selected appropriately, such as the bell-shaped function $\mu A_q(x)$ or $\mu B_q(y)$.

$$\mu A_q(x) = \exp\left[-\left(\frac{x - c_q}{a_q}\right)^2\right], q = 1,2 \tag{36}$$

$$\mu B_q(y) = \exp\left[-\left(\frac{y - c_q}{a_q}\right)^2\right], q = 1,2 \tag{37}$$

where a_q and c_q are premise parameters.

Layer^2: Nodes are indicated by circles and labeled with "Π" in Figure 13. It takes layer^1's outputs as input and multiplies them to yield weight. The output of layer^2 can be showed as follows:

$$O_{2,q} = w_q = \mu A_q(x) \times \mu B_q(y) \tag{38}$$

Layer^3: Each output function is calculated by normalizing the weight of a certain node by comparing with the weights of other nodes.

$$O_{3,q} = \overline{w_q} = \frac{w_q}{w_q + w_q}, q = 1,2 \tag{39}$$

Layer^4: Each node q of this layer is an adaptive node.

$$O_{4,q} = \overline{w_q} f_q = \overline{w_q}(p_q x + s_q y + r_q), q = 1,2 \tag{40}$$

where r_q represents bias and p_q and s_q indicate consequent parameters.

Layer^5: This is the convergence layer. It calculates the total of rules and yields a single output.

$$O_{5,q} = \sum_q \overline{w_q} f_q = \frac{\sum_q w_q f_q}{\sum_q w_q}, q = 1,2 \tag{41}$$

In this paper, the output of the ANFIS is $\hat{v}_i(k-1)$, the input vector is $x_i(k-1) = [y(k-1), \ldots, y(k-in_a)$, $= [\varphi_1, \varphi_2, \ldots \varphi_m]$, and the membership function of ANFIS can be expressed as follows:

$$p_{ij}[\varphi_i(k-1)] = exp\left\{-\frac{\left[\varphi_i(k-1) - c_{ij}\right]^2}{2(\sigma_{ij})^2}\right\} \tag{42}$$

where p_{ij} is the connection weights and σ_{ij} and c_{ij} are the width and center of the membership function. Expressing the i fuzzy rule is accomplished as follows [41]:

R^r: if φ_1 is A^r_{1j}, φ_2 is A^r_{2j}, ..., and φ_m is $A^r_{\mathrm{m}j}$, then

$$\phi_r(k) = \sum_{i=0}^{m} p^r_{ij} \varphi_i(k) \tag{43}$$

According to Ref. [42], the estimate $\hat{v}_i(k-1)$ is as follows and the estimation algorithm structure of virtual unmodeled dynamics is in Figure 14.

$$\hat{\mathrm{v}}_\mathrm{i}(\mathrm{k}-1) = \sum_{\mathrm{r}=1}^{\mathrm{m}} \overline{\mathrm{w}}_\mathrm{r}(\mathrm{k}-1)\phi_\mathrm{r}(\mathrm{k}-1), \mathrm{l} = 1,2,\cdots,\mathrm{m} \tag{44}$$

where $\overline{w}_r(k-1) = \frac{w_r(k-1)}{\sum_{r=1}^{m} w_r(k-1)}$, $w_r(k-1) = \prod_{i=1}^{m} p_{ij}[\varphi_i(k-1)]$. The parameters c_{ij} and σ_{ij} are adjusted by estimate error $|v_i(k-1) - \hat{v}_i(k-1)|$.

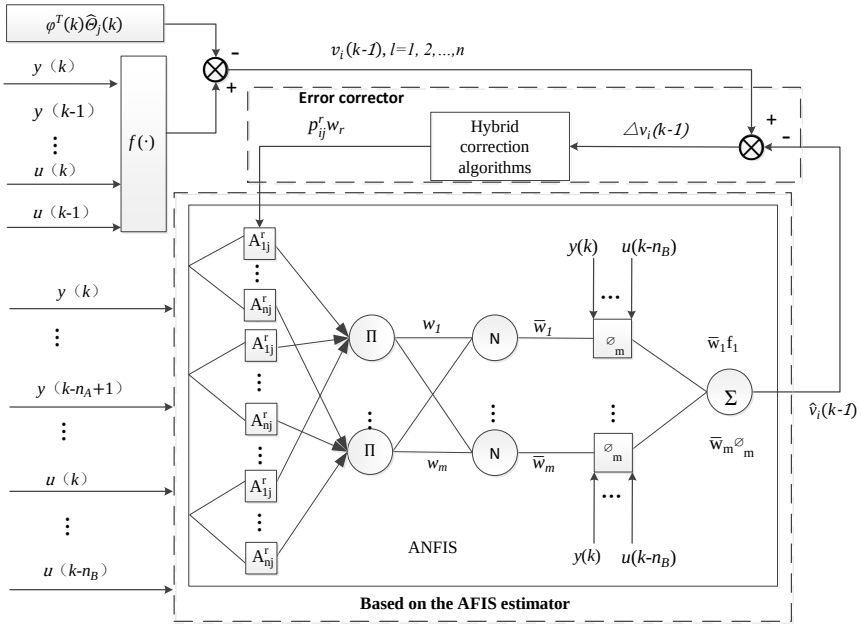

Figure 14. Estimation algorithm structure of virtual unmodeled dynamics $\hat{v}_i(k-1)$.

6. Simulation Results

To validate the effectiveness of the present method, the nonlinear adaptive control strategy was applied to the nutrient solution pH value system. In this paper, two kinds of experiments were carried out in the simulation research: (1) A setpoint tracking experiment was devised to examine the tracking effect of the present method. (2) A parameter uncertainty experiment was devised to investigate the control performance under the condition of time-varying parameters. (3) A noise and unmeasurable disturbances experiment was devised to validate the feasibility of the nonlinear adaptive strategy.

(1) Setpoint tracking experiment. To further illustrate the availability and feasibility of the method put forward in this paper, the pH scale was designed to be adjusted from 3 to 10. The experimental design is outlined as follows. The pH setpoint of the nutrient solution was changed every 10 min during a 50 min experimental process. The set value of the pH is changed from 3.3 to 4.5 at t = 0–10 min and then was designed from 4.5 to 6.8 at 10–20 min. Subsequently, the setpoint of pH was changed from 6.8 to 9.5 at t = 20–30 min. In the end, the set value of pH was changed from 9.5 to 7.2 at t = 30–50 min.

The initial parameters of the model are given as follows: x_a = 0.36 mol/L, x_b = 0.1 mol/L, Q_a = 1.0 L/min, v = 500 L, Q_f = 0.5 L/min, C_f = 0.1 mol/L, Q_s = 1.5 L/min, and C_s = 0.1 mol/L. The initial working point is as follows: u = 3.42 L/min and y = 3.3; the open-loop step experiment was carried out at this working point to obtain the experimental data, and the system order is expressed as $n_a = 2$, $n_b = 1$. The model of the system is obtained around the working point through system identification: $A(z^{-1}) = 1 - 1.926z^{-1} + 0.9926z^{-2}$, $B(z^{-1}) = 0.5891 - 0.5877z^{-1}$. The parameters of the nonlinear adaptive controller are designed as follows: λ = 0.1, the parameters of switching criterion $C = 1, T = 2, \Delta = 0.001$. The membership function of ANFIS is arranged as the Gaussian function which the training time is set to 40. The input of ANFIS is divided into three fuzzy intervals.

In comparison, the gain-scheduling PID control method was adopted in this process. The experiments were devised as follows. The pH setpoint of the nutrient solution was changed every 50 min due to the long adjustment time for the PID control method. The set value of the pH was changed from 3.1 to 4.5 at t = 0–50 min and then was designed from 4.5 to 6.8 at 50–100 min. Subsequently, the setpoint of the pH was changed from 6.8 to 9.5 at t = 100–150 min. In the end, the set value of the pH was changed from 9.5 to 7.2 at t = 150–250 min. In this paper, the classic incremental PID structure is applied to the nutrient solution and the PID controller as follows:

$$u(t) = u(t-1) + K_p[e(t) - e(t-1)] + K_I e(t) + K_d[e(t) - 2e(t-1) + e(t-2)] \quad (45)$$

where

$$e(t) = w(t) - y(t) \quad (46)$$

K_p, K_I, and K_d denote the proportional gain, integral gain, and derivative gain, respectively.

To mitigate the impact of nonlinearity and varying dynamics on the system, the gain-scheduling PID strategy was applied to the process by modifying the proportional, integral, and derivative gains in specific operating conditions. The parameters of the PID controller are provided in Table 2 at different operating points.

Table 2. The parameters of the gain-scheduling PID controller.

Operating Points	K_p	K_I	K_d
pH = 4.5	0.0003	0.000012	0
pH = 6.8	0.00025	0.000015	0
pH = 9.5	0.0005	0.00005	0
pH = 7.2	0.0004	0.000015	0

(2) Parameters uncertainty experiment. In fact, the parameters, such as acid flow rate, are very difficult to be obtained precisely in advance and may vary with different operation conditions on the basis of actual production for the nutrient solution. To prove the effectiveness of the present method, the abovementioned parameters were changed during the experiment when the system was in steady-stage. The experimental design is outlined as follows. Acid flow was changed from 1.0 to 1.1 L at t = 33 min. The gain-scheduling PID control method was also adopted here for comparison. The changes in the parameter amplitude were similar to the above experiment and were designed as follows. The acid flow was changed from 1.0 to 1.1 L at t = 158 min.

(3) Noise and unmeasurable disturbances experiment. As a matter of fact, the actual process has noise and additional unmeasurable interferences in the plant factory. The acidity and alkalinity concentrations are difficult to detect in real-time in practical systems. The above factors belong to unmeasurable disturbances. Moreover, to further prove the feasibility of the present method, the noise was also added for testing purposes during the experiment when the system was in steady-stage. The experimental design is outlined as follows. The acidity and alkalinity concentrations were added random disturbances with amplitudes ranging from [−0.05 +0.05] around their operating point at t = 35 min. The noise was added to the pH measurement with amplitudes ranging from [−0.1 +0.1] at t = 42.5 min. The gain-scheduling PID control method is also adopted here for comparison. The acidity and alkalinity concentrations were added random disturbances with amplitudes ranging from [−0.05 +0.05] around their operating point at t = 170 min. The noise was added to the pH measurement with amplitudes ranging from [−0.1 +0.1] at t = 210 min.

Figures 15–20 display the simulation results. Figures 15–18 show the control effect using a gain-scheduling PID control strategy, and Figures 18–20 show the control effect by nonlinear adaptive control strategy. The gain-scheduling PID control strategy does not produce a desirable control effect, as can be observed. Due to the uncertainties and strong nonlinearity in the nutrient solution system, the pH value has a long adjustment time and reaches the steady state very slowly, especially at the setpoint of 4.5 and 9.5. However, the adjustment time of the nonlinear adaptive control strategy is short and reaches the steady state within 5 min. In additional, the pH has small overshoot, which greatly enhances the control effect of the system.

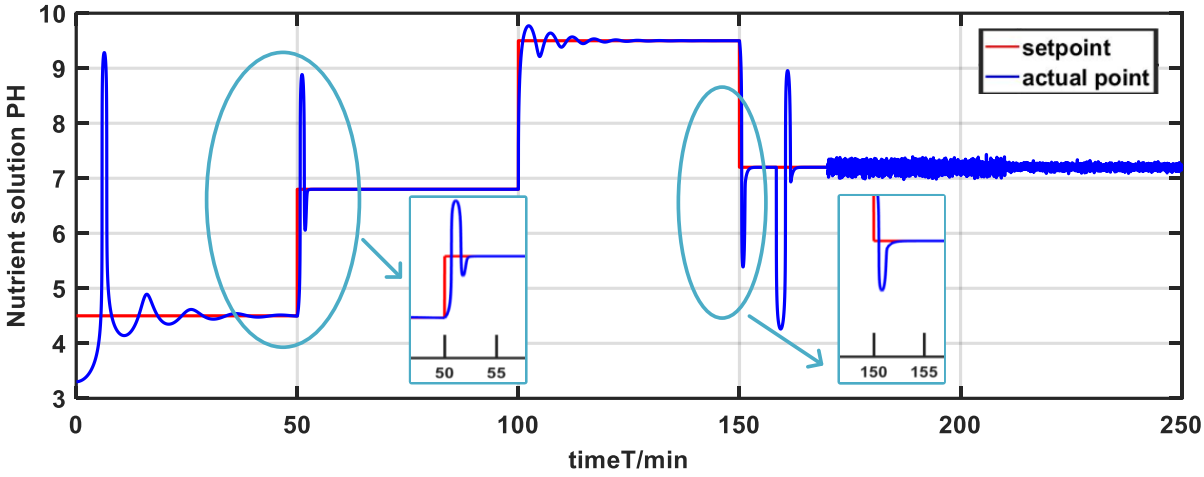

Figure 15. The related response of pH setpoint for gain-scheduling PID control.

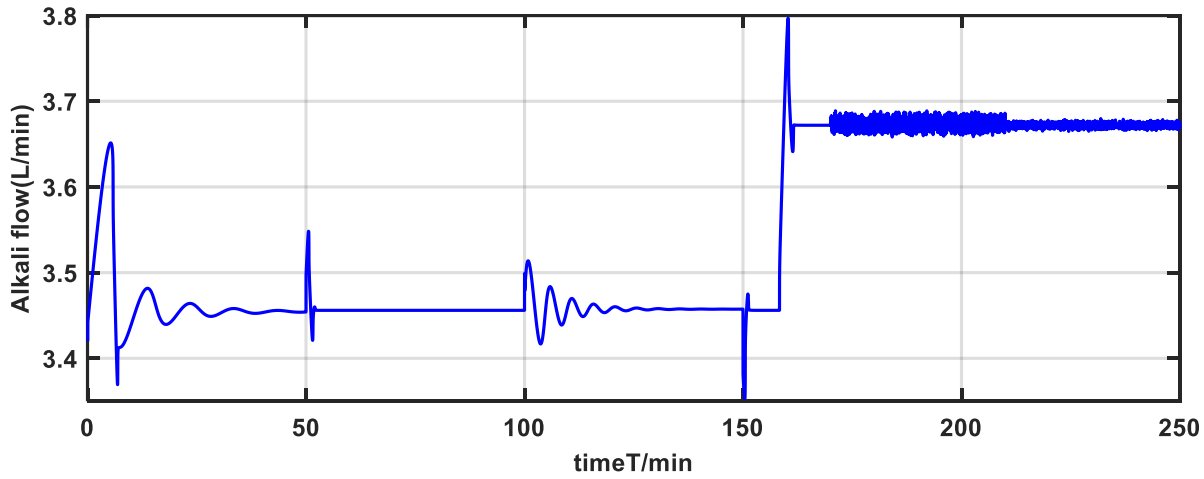

Figure 16. The related response of control input for gain-scheduling PID control.

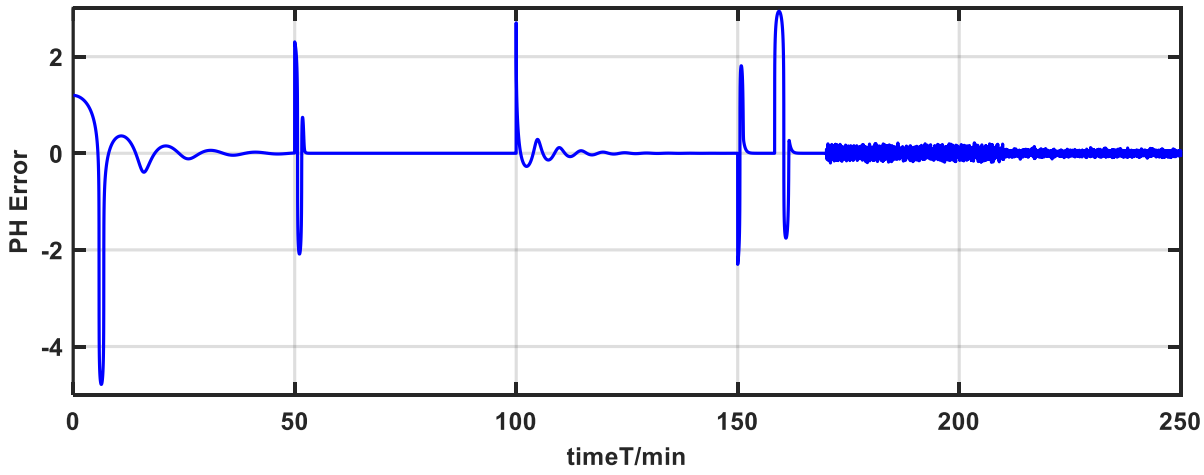

Figure 17. The pH error value of gain-scheduling PID control.

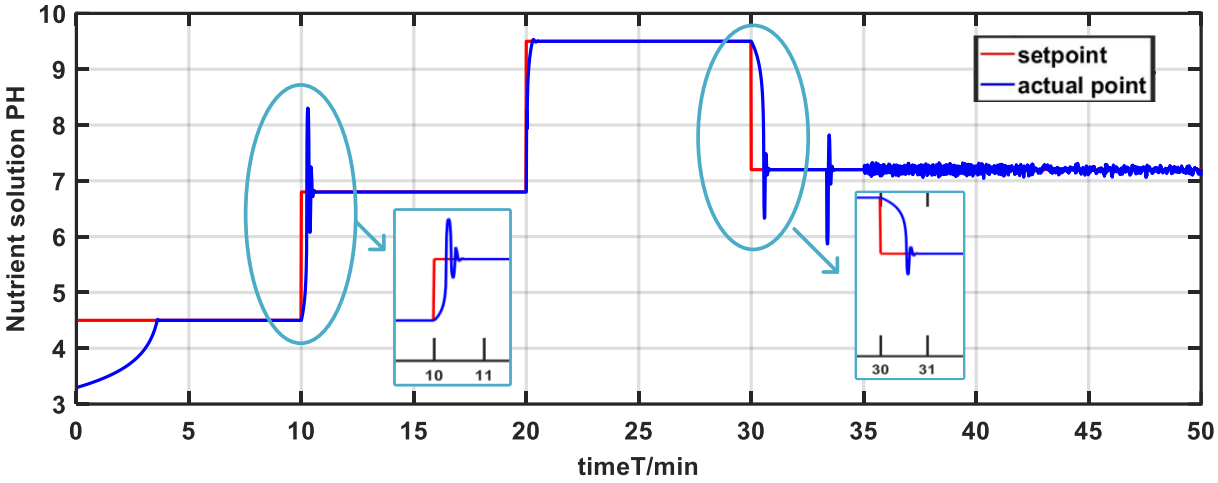

Figure 18. The corresponding response of pH setpoint for nonlinear adaptive control.

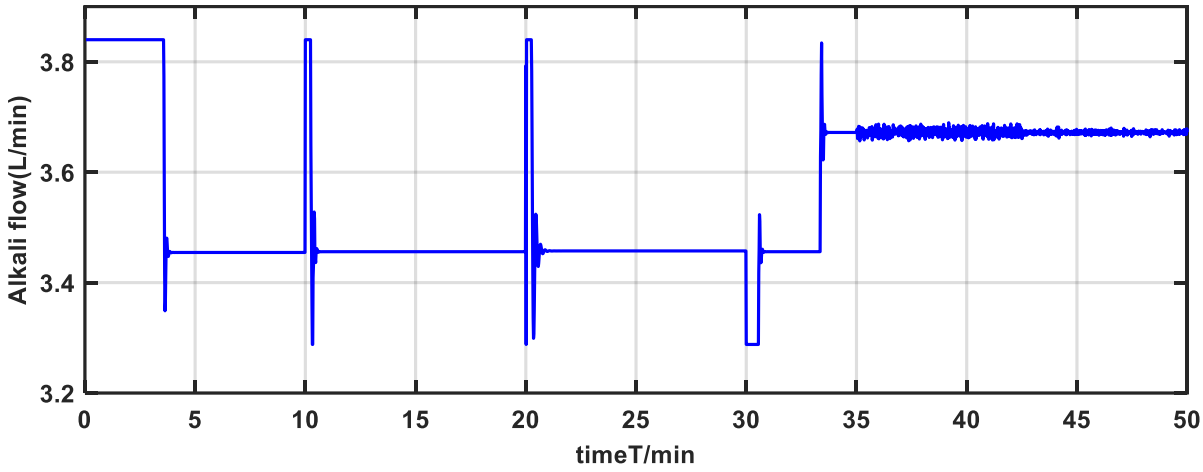

Figure 19. The corresponding response of control input for nonlinear adaptive control.

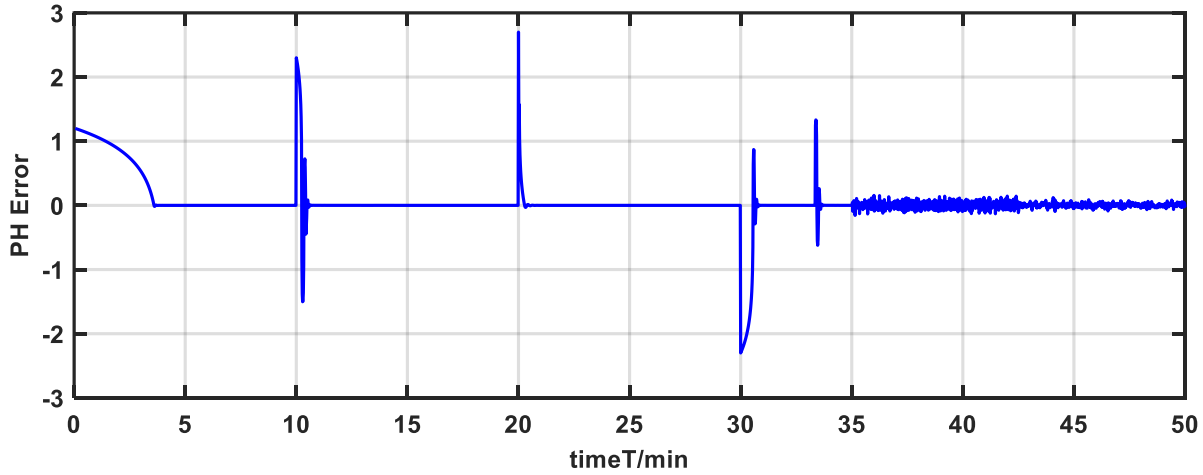

Figure 20. The pH error value for nonlinear adaptive control.

Regarding the situation of parameter uncertainties, the pH value features large fluctuations based on the gain-scheduling PID control strategy from Figure 15. However, as depicted in Figure 18, the pH value undergoes less fluctuations and rapidly adjusts towards the setpoint during parameter variations. Therefore, the pH is capable of fast setpoint tracking and mitigating the effects of uncertainties on the system.

Concerning the situation of noise and unmeasurable disturbances, the proposed method has good robustness similar to the gain-scheduling PID controller, as depicted in Figure 18. Therefore,

the nonlinear adaptive controller is not sensitive to interference and noise. The precise control of pH for the nutrient solution can adjust the acidity or alkalinity of the nutrient solution to regulate the solubility and stability of the nutrients, thereby promoting nutrient absorption and utilization, maintaining healthy root development, and, ultimately, enhancing crops yield.

To further substantiate the control performance of the nonlinear adaptive control strategy, the average error and standard error are selected to measure the control effect. The formula for calculating the average error and standard error is as follows and the results of two methods are show in Table 3.

$$\eta = \frac{1}{n}\sum_{i=1}^{n}|x_i - \overline{x}| \tag{47}$$

$$\tau = \sqrt{\frac{1}{n}\sum_{i=1}^{n}|(x_i - \overline{x})^2|} \tag{48}$$

Table 3. Performance comparison between gain-scheduling PID controller and nonlinear adaptive controller.

Methods	Nutrient Solution pH Error	
	Mean	Standard
Gain-scheduling PID	0.1338	0.4784
Nonlinear adaptive control	0.1046	0.3009

The above table shows the average error and standard error of the gain-scheduling PID control strategy and the nonlinear adaptive control strategy, respectively. The average error and standard error of the gain-scheduling PID control strategy are 0.1338 and 0.4784, respectively. The average error and standard error of the nonlinear adaptive control strategy are 0.1046 and 0.3009, respectively.

By comparing with two control strategies, it can be deduced that the nonlinear adaptive control strategy has a good control effect on the actual nutrient solution pH in many aspects. For one thing, the nonlinear adaptive controller enhances the setpoint tracking performance that shortens the adjustment time and decreases overshoot; for another, it has a better adaptability of parameter uncertainties. Therefore, the proposed method can improve the dynamic performance and has good robustness in the face of strong nonlinearity and parameters uncertainty.

The setpoint tracking experiment, the parameters uncertainty experiment, and the noise and unmeasurable disturbances experiments are conducted to validate the effectiveness and feasibility of the proposed control method for the plant factory. Precisely regulating the pH value under various complex situations promotes nutrient transformation and metabolism, improving crops' nutrient utilization efficiency while creating a suitable environment for plant growth. Furthermore, it can reduce nutrient waste and loss, increasing crops yield and thereby enhancing the economic efficiency of plant factories.

7. Conclusions

According to the actual process of nutrient solutions, this paper constructs a dynamic model of the pH of nutrient solutions based on the law of acid–base balance. To address the complex dynamic characteristics of strong nonlinearity and parameter uncertainty of the model, a nonlinear adaptive generalized predictive control method based on ANFIS is put forward. The setpoint tracking experiment and parameters uncertainty experiment were devised. For the PID control strategy, the mean error and standard error are 0.1338 and 0.4784, respectively. In comparison, the nonlinear controller has a significant enhancement, with the results of 0.1046 and 0.3009 corresponding to the mean and standard error. The experiments' results show that the presented method can track the set value quickly. Moreover, the pH undergoes less fluctuations and achieves a better control effect compared to the gain-scheduling PID controller in the presence of the parameter uncertainties. Therefore, the proposed control strategy can provide the suitable growth environment, promoting healthy crops' growth and enhancing the economic efficiency.

Author Contributions: Y.W., N.Z., C.C., Y.J. and T.L. conceived and designed the experiments. Y.W. and N.Z. performed the experiments. Y.W. and N.Z. analyzed the data. Y.W. and N.Z. supervised

the experiment. Y.W. and N.Z. wrote the manuscript. Y.W., N.Z., C.C., Y.J. and T.L. reviewed the manuscript. All authors have read and agreed to the published version of the manuscript.

Funding: This project was supported by the National Natural Science Foundation of China (NSFC) (61673281, 61903264), the Scientific Research Funding Project of Liaoning Province, China (LJKZ0689), the Natural Science Foundation of Liaoning Province (2019-KF-03-01), and the National Key Research and Development Program "Key Special Project on Intergovernmental Cooperation for National Scientific and Technological Innovation" (2019YFE0197700). Project of Liaoning Provincial Department of Education (LJKMZ20221035).

Data Availability Statement: Data are unavailable due to privacy.

Acknowledgments: The authors sincerely thank the National Natural Science Foundation of China for their financial support.

Conflicts of Interest: The authors declare no conflict of interest.

References

1. Zhang, Y.; Kacira, M.; An, L. A CFD study on improving air flow uniformity in indoor plant factory system. *Biosyst. Eng.* **2016**, *147*, 193–204. [CrossRef]
2. Santiteerakul, S.; Sopadang, A.; Tippayawong, K.Y.; Tamvimol, K. The Role of Smart Technology in Sustainable Agriculture: A Case Study of Wangree Plant Factory. *Sustainability* **2020**, *12*, 4640. [CrossRef]
3. Kozai, T. Towards sustainable plant factories with artificial lighting (PFALs) for achieving SDGs. *Int. J. Agric. Biol. Eng.* **2019**, *12*, 28–37. [CrossRef]
4. Xu, K.; Kitazumi, Y.; Kano, K.; Shirai, O. Construction of an Automatic Nutrient Solution Management System for Hydroponics-Adjustment of the K^+-Concentration and Volume of Water. *Anal. Sci.* **2019**, *35*, 595–598. [CrossRef] [PubMed]
5. Huo, S.; Liu, J.; Min, A.; Chen, P.; Necas, D.; Cheng, P.; Ruan, R. The influence of microalgae on vegetable production and nutrient removal in greenhouse hydroponics. *J. Clean. Prod.* **2019**, *243*, 118563. [CrossRef]
6. Wada, T. Theory and Technology to Control the Nutrient Solution of Hydroponics. In *Plant Factory Using Artificial Light*; Elsevier: Amsterdam, The Netherlands, 2019; pp. 5–14.
7. Wang, M.; Dong, C.; Gao, W. Evaluation of the growth, photosynthetic characteristics, antioxidant capacity, biomass yield and quality of tomato using aeroponics, hydroponics and porous tube-vermiculite systems in bio-regenerative life support systems. *Life Sci. Space Res.* **2019**, *22*, 68–75. [CrossRef]
8. Domingues, D.S.; Takahashi, H.W.; Camara, C.; Nixdorf, S.L. Automated system developed to control pH and concentration of nutrient solution evaluated in hydroponic lettuce production. *Comput. Electron. Agric.* **2012**, *84*, 53–61. [CrossRef]
9. Custos, J.M.; Moyne, C.; Sterckeman, T. How root nutrient uptake affects rhizosphere pH: A modelling study. *Geoderma* **2020**, *369*, 114314. [CrossRef]
10. Loh, A.P.; De, D.S.; Krishnaswamy, P.R. pH and Level Controller for a pH Neutralization Process. *Ind. Eng. Chem. Res.* **2001**, *40*, 3579–3584. [CrossRef]
11. Wright, R.A.; Kravaris, C. Nonlinear control of pH processes using the strong acid equivalent. *Ind. Eng. Chem. Res.* **1991**, *30*, 1561–1572. [CrossRef]
12. Kim, K.-S.; Kwon, T.-I.; Yeo, Y.-K. Experimental Evaluation of Bilinear Model Predictive Control for pH Neutralization Processes. *J. Chem. Eng. Jpn.* **2000**, *33*, 285–291. [CrossRef]
13. Akin, H.; Brandam, C.; Meyer, X.M.; Strehaiano, P. A model for pH determination during alcoholic fermentation of a grape must by Saccharomyces cerevisiae. *Chem. Eng. Process.* **2008**, *47*, 1986–1993. [CrossRef]
14. Stebel, K.; Metzger, M. Distributed parameter model for pH process including distributed continuous and discrete reactant feed. *Comput. Chem. Eng.* **2012**, *38*, 82–93. [CrossRef]
15. Czeczot, J. Robust Control of pH Process on the Basis of the B-BAC Mathodology. *IFAC Proc. Vol.* **2003**, *36*, 437–442. [CrossRef]
16. Liu, Y.-J.; Li, J.; Tong, S.; Chen, C.L.P. Neural Network Control-Based Adaptive Learning Design for Nonlinear Systems with Full-State Constraints. *IEEE Trans. Neural Netw. Learn. Syst.* **2016**, *27*, 1562–1571. [CrossRef]
17. Xu, D.; Ahmed, H.A.; Tong, Y.; Yang, Q.; van Willigenburg, L.G. Optimal control as a tool to investigate the profitability of a Chinese plant factory—Lettuce production system. *Biosyst. Eng.* **2021**, *208*, 319–332. [CrossRef]
18. Liu, J.; Li, X.; Li, J.; Wang, K.; Wang, F.; Cui, G. Model-Free Adaptive Control of pH Value of Wet Desulfurization Slurry under Switching of Multiple Working Conditions. *Complexity* **2020**, *2020*, 4727412. [CrossRef]
19. Yaez-Badillo, H.; Beltran-Carbajal, F.; Tapia-Olvera, R.; Favela-Contreras, A.; Sotelo, C.; Sotelo, D. Adaptive Robust Motion Control of Quadrotor Systems Using Artificial Neural Networks and Particle Swarm Optimization. *Mathematics* **2021**, *9*, 2367. [CrossRef]
20. Kalafatis, A.D.; Wang, L.; Cluett, W.R. Linearizing feedforward–feedback control of pH processes based on the Wiener model. *J. Process Control* **2005**, *15*, 103–112. [CrossRef]
21. Wu, H.; Yan, F.; Wang, G.; Lv, C. A predictive control based on decentralized fuzzy inference for a pH neutralization process. *J. Process Control* **2022**, *110*, 76–83. [CrossRef]

22. Heredia-Molinero, M.C.; Sánchez-Prieto, J.; Briongos, J.V.; Palancar, M.C. Feedback PID-like fuzzy controller for pH regulatory control near the equivalence point. *J. Process Control* **2014**, *24*, 1023–1037. [CrossRef]
23. Biagiola, S.I.; Agamennoni, O.E.; Figueroa, J.L. Robust Control of Wiener Systems: Application to A pH Neutralization Process. *Braz. J. Chem. Eng.* **2016**, *33*, 145–153. [CrossRef]
24. Lin, Q.; Loxton, R.; Teo, K.L. The control parameterization method for nonlinear optimal control: A survey. *J. Ind. Manag. Optim.* **2017**, *10*, 275–309. [CrossRef]
25. Shan, Y.; Zhang, L.; Ma, X.; Hu, X.; Hu, Z. Application of the Modified Fuzzy-PID-Smith Predictive Compensation Algorithm in a pH-Controlled Liquid Fertilizer System. *Processes* **2021**, *9*, 1506. [CrossRef]
26. Hermansson, A.W.; Syafiie, S. Model predictive control of pH neutralization processes: A review. *Control. Eng. Pract.* **2015**, *45*, 98–109. [CrossRef]
27. Seminar, K.; Chadirin, Y.; Setiawan, B. Development of a pH Control System for nutrient solution in EBB and Flow. Hydroponic Culture Based on Fuzzy Logic. *IFAC Proc. Vol.* **2001**, *34*, 87–90.
28. Su, C.; Li, P. Adaptive predictive functional control based on Takagi-Sugeno model and its application to pH process. *J. Cent. South Univ. Technol.* **2010**, *17*, 363–371. [CrossRef]
29. Yao, D.; Dou, C.; Yue, D.; Zhao, N.; Zhang, T. Adaptive neural network consensus tracking control for uncertain multi-agent systems with predefined accuracy. *Nonlinear Dyn.* **2020**, *101*, 2249–2262. [CrossRef]
30. Yan, K.; Chen, C.; Xu, X.; Wu, Q. Neural network-based output feedback fault tolerant tracking control for nonlinear systems with unknown control directions. *Complexity* **2022**, *2022*, 4770439. [CrossRef]
31. Wang, Y.; Chai, T.; Fu, J.; Sun, J.; Wang, H. Adaptive Decoupling Switching Control of the Forced-Circulation Evaporation System Using Neural Networks. *IEEE Trans. Control. Syst. Technol.* **2013**, *21*, 964–974. [CrossRef]
32. Zhang, L.; Zhang, D.; Nguang, S.K.; Swain, A.K.; Yu, Z. Event-Triggered Output-Feedback Control for Synchronization of Delayed Neural Networks. *IEEE Trans. Cybern.* **2022**, 1–13. [CrossRef] [PubMed]
33. Niu, Y.; Zhang, K. Cloud Model-based Reasoning for Control of Nutrient Solution pH in Fertilization Machine. *J. Agric. Mach.* **2016**, *47*, 57–64+72.
34. Yang, Y.; Chen, Y.; Wang, Y.; Li, C.; Li, L. Modelling a combined method based on ANFIS and neural network improved by DE algorithm: A case study for short-term electricity demand forecasting. *Appl. Soft Comput.* **2016**, *49*, 663–675. [CrossRef]
35. Qiu, W.; Liu, X.; Li, H. A generalized method for forecasting based on fuzzy time series. *Expert. Syst. Appl.* **2011**, *38*, 10446–10453. [CrossRef]
36. Hog, B.W.; El-Rabaie, N.M. Multivariable generalized predictive control of a boiler system. *IEEE Trans. Energy Convers.* **1991**, *6*, 282–288. [CrossRef]
37. Levie, R.D. *Aqueous Acid-Base Equilibria and Titrations*; Oxford University Press: Oxford, UK, 1999.
38. Du, J.; Song, C.; Li, P. Multilinear model control of Hammerstein-like systems based on an included angle dividing method and the MLD-MPC strategy. *Ind. Eng. Chem. Res.* **2012**, *48*, 3934–3943. [CrossRef]
39. Du, J.; Johansen, T.A. Integrated Multimodel Control of Nonlinear Systems Based on Gap Metric and Stability Margin. *Ind. Eng. Chem. Res.* **2014**, *53*, 10206–10215. [CrossRef]
40. Zhu, K.Y.; Qin, X.F.; Chai, T.Y. A New Decoupling Design of Self-tuning Multivariable Generalized Predictive Control. *Int. J. Adapt. Control. Signal Process.* **1999**, *13*, 183–196. [CrossRef]
41. Zhang, H.; Quan, Y. Modeling, identification, and control of a class of nonlinear systems. *IEEE Trans. Fuzzy Syst.* **2001**, *9*, 349–354. [CrossRef]
42. Zhang, Y.; Chai, T.; Wang, H. A Nonlinear Control Method Based on and Multiple Models for a Class of SISO Nonlinear Systems and Its Application. *IEEE Trans. Neural Netw.* **2011**, *22*, 1783–1795. [CrossRef]